Neurochem Res (2015) 40:1042–1052
DOI 10.1007/s11064-015-1561-x

ORIGINAL PAPER

Up-regulation of VCAM1 Relates to Neuronal Apoptosis After Intracerebral Hemorrhage in Adult Rats

Dongmei Zhang[1] · Damin Yuan[2] · Jianhong Shen[3] · Yaohua Yan[3] · Chen Gong[4] · Jun Gu[3] · Huaqing Xue[5] · Yuhang Qian[5] · Weidong Zhang[6] · Xiaojuan He[7] · Li Yao[8] · Yuhong Ji[2] · Aiguo Shen[4,5]

Received: 28 June 2014 / Revised: 18 March 2015 / Accepted: 21 March 2015 / Published online: 14 April 2015
© Springer Science+Business Media New York 2015

Abstract Vascular cell adhesion molecule 1 (VCAM1) is a member of the Immunoglobulin superfamily and encodes a cell surface sialoglycoprotein expressed in cytokine-activated endothelium. This type I membrane protein mediates leukocyte-endothelial cell adhesion, facilitates the downstream signaling, and may play a role in the development of artherosclerosis and rheumatoid arthritis. Accumulating evidence has demonstrated that VCAM1 exerts an anti-apoptotic effect in several tumor tissues such as ovarian cancer and breast cancer. Intracerebral hemorrhage (ICH) is the second most common subtype of stroke with high morbidity and mortality, which imposes a big burden on individuals and the whole society. These together prompted us to question whether VCAM1 has some association with neuron apoptosis during the pathological process of ICH. An ICH rat model was established and assessed by behavioral tests in order to explore the role of VCAM1 after ICH. Up-regulation of VCAM1 was observed in brain areas surrounding the hematoma following ICH by western blotting and immunohistochemistry. Immunofluorescence manifested VCAM1 was strikingly increased in neurons, but not in astrocytes and microglia. Furthermore, we detected that neuronal apoptosis marker active caspase-3 had co-localizations with VCAM1. At the same time, Bcl-2 was also co-localized with VCAM1. Taken together, our findings suggested that VCAM1 might be involved in the neuronal apoptosis and pathophysiology of ICH.

Keywords Intracerebral hemorrhage (ICH) · VCAM1 · Apoptosis · Adult rats

Introduction

The global burden of acute spontaneous (nontraumatic) intracerebral hemorrhage (ICH) seem unchanged over the past quarter century [1, 2], in spite of the improvements in outcome that can be acquired by organized stroke unit care and neurosurgical hematoma evacuation [3]. In the process of ICH, rapid accumulation of blood in brain parenchyma leads to

Dongmei Zhang and Damin Yuan are co-first authors.

✉ Yuhong Ji
yuhongji163@163.com

✉ Aiguo Shen
shen_aiguo@yahoo.com

Damin Yuan
yuandamin99@163.com; 476490163@qq.com

[1] Department of Pathogen Biology, Medical College, Jiangsu Province Key Laboratory for Inflammation and Molecular Drug Target, Nantong University, Nantong 226001, China

[2] Department of Immunology, Medical College, Nantong University, Nantong 226001, China

[3] Department of Neurology, Affiliated Hospital of Nantong University, Nantong 226001, China

[4] Co-innovation Center of Neuroregeneration, Nantong University, Nantong 226001, China

[5] Jiangsu Key Laboratory of Neuroregeneration, Nantong University, Nantong 226001, China

[6] Department of Orthopaedics, Affiliated Mental Health Center of Nantong University, Nantong 226001, China

[7] Department of Pathology, Medical College, Nantong University, Nantong 226001, China

[8] Department of Immunology, Medical College, Jiangnan University, Wuxi 214122, China

disruption of normal anatomy and increased local pressure [4, 5]. ICH is an often fatal type of stroke that kills a large number of people all around the world. If the patient survives the ictus, the resulting hematoma within brain parenchyma will trigger a succession of adverse events leading to secondary insults and severe neurological deficits. Although multiple resources have been thrown into clinical and basic researches, the prognosis of ICH patients remains poor [6]. The primary damage is caused by the dynamic of hematoma expansion associated with mass effect; and the secondary damage consists of many parallel pathways including cytotoxicity of blood, inflammation, oxidative stress, and so on. Together, primary and secondary damages lead up to a neuronal injury, and ultimately cause disability or even the death [7]. Neuronal apoptosis, astrocytic proliferation and oligodendrocytic death have been involved in these processes [8–10]; and among them, neuronal apoptosis is counted as one of the most crucial events which includes sophisticated anti-apoptotic and subtle pro-apoptotic modulation. Apoptosis is mostly regulated by the B cell leukemia-2 gene product Bcl-2 family (Bcl-2, Bcl-x, Bax, Bak and Bad) and the caspase family (ICH-1 and CPP32), with apoptosis being resist by Bcl-2 and Bcl-x, and promoted by Bax, Bak, Bad, ICH-1 and CPP32 [11]. Apoptosis, a physiological program of cellular death, can be separated into extrinsic pathway and intrinsic pathway. The first mentioned of two is initiated by ligation of death receptors, the recruitment and activation of caspase-8 at the receptor complexes, while the latter is mitochondria-dependent mechanism, related with the release of cytochrome c and activation of caspases [12]. Meanwhile, caspase-3 is a major executioner caspase and can be continually activated during both pathways. Although multiple researches have focused on the mechanisms underlying ICH, we merely have understood a sketchy knowledge of the molecular and cellular mechanisms, and still more work should be done to realize the pathological progress and to improve in the further treatment of ICH.

Vascular cell adhesion molecule 1 (VCAM1), also known as CD106, is a member of the immunoglobulin (Ig) superfamily [13]. It is a cell surface sialoglycoprotein first discovered on cytokine-activated endothelium [14]. VCAM1 is important in cell–cell recognition, functions in leukocyte-endothelial cell adhesion, interacts with the beta-1 integrin VLA4 on leukocytes, and mediates both cell adhesion and the downstream signal transduction. The VCAM1/VLA4 interaction plays a pathophysiologic role both in immune responses and in leukocyte emigration to sites of inflammation. What's more, VCAM-1 reportedly protects breast cancer cells, human myeloma cell lines, and colon cancer cells from apoptosis [15–17]. Nonetheless, the relationship between VCAM1 and neuronal apoptosis following ICH are still being appreciated. The process of apoptosis is governed by both pro-apoptotic and anti-apoptotic proteins p53, a tumor-suppressor protein that has the pro-apoptotic effect, is inactivated and degraded under normal conditions, whereas different pathologic stimulican can induce the expression of p53 [18]. The raised levels of p53 result in pro-apoptotic responses by a combination of gene activation (e.g. p21WAF1 and Bax) and gene repression (e.g. Bcl-2). Bcl-2, Bcl-xL and Bax are members of the Bcl-2 family, which are crucial regulators of apoptosis. Bcl-2 is a key survival molecule. As VCAM1 participates in multiple cellular activities, whether it takes part in the pathophysiologic processes following ICH remains to be researched.

So far, we know little about the functions of VCAM1 in CNS after ICH. Since VCAM1 is involved in apoptosis, we assumed that VCAM1 might contribute to the secondary injury following ICH, and associate with neuronal apoptosis. Our study explored for the first time about the expression and distribution of VCAM1 in rat brain after ICH, which manifested the potential role of VCAM1 in the pathophysiological process of apoptosis after ICH. This study was implemented to gain a progress into the function of VCAM1 in the adult CNS and might lay a solid foundation for further research incase to be applied to clinical treatment for its role in injury and repair after ICH.

Materials and Methods

Animals and the ICH Model

All experiments were executed in accordance with the National Institutes of Health Guidelines for the Care and Use of Laboratory Animals (National Research Council, 1996, USA); all animal procedures were approved by the Chinese National Committee to the Use of Experimental Animals f or Medical Purposes, Jiangsu Branch. Adult male Sprague–Dawley rats with an average weight of 250 g were employed in this study. The rats were anesthetized intraperitoneally with sodium pentobarbital (50 mg/kg) and then placed in a stereotaxic frame. Near the right coronal suture 3.5 mm lateral to the midline, we drilled a cranial burr hole (1 mm in diameter). Autologous whole blood (50 μL) was converged by cutting the tail tip with a pair of scissors, and drawing 50 μL blood into a sterile syringe [19]. The syringe was inserted stereotaxically into the right caudate putamen (coordinates: 0.2 mm anterior, 5.5 mm ventral, and 3.5 mm lateral to the bregma), and the autologous blood injected at the rate of 10 μL/min [20]. Following injection, the needle was fixed for over 10 min before being removed. Ketoprofen (5 mg/kg) was executed to minimize postsurgical pain and discomfort. After all the manipulations, rats were permitted to return to their cages and allowed freely to get the food and water. Experimental animals ($n = 3$ per time point) were

sacrificed to extract the protein for western blot analysis at 3 h, 6 h, 12 h, 1, 2, 3, 5, and 7 day(s) following ICH, respectively. Normal rats (n = 3) and sham-controlled rats (n = 3) were killed on the third day. Additional experimental animals (n = 2 per time point) for sections were killed at each time point for pathologic studies. All efforts were made to minimize the number of animals used and their suffering.

Behavioral Testing Procedures

Forelimb Placing Test

The rats were held by the torsos, enabling the forelimb to hang free. Independent testing of each forelimb was elicited by brushing the respective vibrissae on the corner edge of a countertop. Intact rats put the forelimb quickly onto the countertop. On the basis of the extent of injury, placing of the forelimb contralateral to the injury may be impaired. In time of the experiments, each rat was tested ten times for each forelimb, and the percentage of trials in which the rat placed the left forelimb was counted [21].

Corner Turn Test

The rats were allowed to performed into a corner, the angle of which was 30 °C. To exit the corner, the rat should turn either to the left or the right, and only the turns involving full rearing along either wall were included (a total of eight per animal). Based on the extent of injury, rats may show a tendency to turn to the side of the injury. The proportion of right turns was used as the corner turn score. And the rats were not picked up instantly after each turn so that they would not expand an aversion for their prepotent turning response [22].

Western Blot Analysis

After injected an overdose of chloral hydrate (10 % solution), rats were executed at different time points postoperatively, and the brain tissue around the hematoma (extending 3 mm to the incision) as well as an equal part of the normal, sham-controlled, and contralateral cortex were dissected out and stored at −80 °C until use. To prepare the lysates, frozen samples were weighed and minced on ice. The samples were then homogenized in lysis buffer (1 % NP-40, 50 mmol/L Tris, pH = 7.5, 5 mmol/L EDTA, 1 % SDS, 1 % sodium deoxycholate, 1 % Triton X-100, 1 mmol/L PMSF, 10 μg/mL aprotinin, and 1 μg/mL leupeptin) and centrifuged at 12,000 rpm and 4 °C for 20 min to collect the supernatant. After ascertain of its protein concentration with the Brad-fordassay (Bio-Rad), protein samples were sustained SDS–polyacrylamide gel electrophoresis (SDS–PAGE) and transferred to a polyvinylidene diflouride filter (PVDF) membrane by a transfer apparatus at 300 mA for 2 h. The membranes were blocked with 5 % non-fat milk for 2 h and incubated with primary antibody against VCAM1 (1:500; Santa Cruz; Sigma-Aldrich), active caspase-3 (1:1000; Cell Signaling), GAPDH (1:1000, Santa Cruz), Bcl-2 (Santa Cruz, 1:500), p53 (1:500; Santa Cruz), and Bax (1:500; Santa Cruz), at 4 °C overnight. At last, the membrane was incubated with a second antibody for 2 h and visualized using an enhanced chemiluminescence system (Pierce Company, USA) [22].

Immunohistochemistry

As the survival times determined, rats were deeply anesthetized and perfused with saline and 4 % paraformaldehyde following through the ascending aorta. After perfusion, the brains were took away and post-fixed in the same fixative for 3 h and then replaced with 20 % sucrose for 2–3 days, followed by 30 % sucrose for 2–3 days. Tissues were then cut at 7 μm with a cryostat. All sections were stored at −20 °C before use. Slide-mounted sections were picked up from the freezer, kept in an oven at 37 °C for 30 min, and rinsed twice in 0.01 M PBS for 5 min. The sections were handled with 10 mmol/L citrate buffer (pH = 6.0) and heated to 121 °C in an autoclave for 3 min to retrieve the antigen. The sections were taken from the pressure cooker and cooled to room temperature spontaneously. Then, we blocked the sections with confining liquid which including 10 % donkey serum, 1 % BSA, 0.3 % Triton X-100 and 0.15 % Tween-20 for 2 h at room temperature, then incubated with anti-VCAM1 antibody (mouse, 1:100, Santa Cruz) overnight at 4 °C. Following incubation in the secondary antibody at 37 °C, the sections were color-reacted with 0.02 % diaminobenzidine tetrahydrochloride (DAB), 0.1 % phosphate buffer solution (PBS), and 3 % H_2O_2. At last, slides were counterstained with hematoxylin, dehydrated, and coverslipped. VCAM1 staining was assessed under a Leica light microscope (Germany). Cells with strong or moderate brown staining were believed as positive; cells with no staining were rated as negative, while cells with weak staining were scored separately.

Double Immunofluorescent Labeling

Additional sets of sections were used for multiple fluorescence staining. After air-dried for 1 h, sections were first blocked with 10 % normal donkey serum blocking solution species the same as secondary antibody, containing 3 % (w/v) bovine serum albumin (BSA), 0.1 % Triton X-100 and 0.05 % Tween 20 for 2 h at room temperature in order to avoid unspecific staining. The sections were then incubated with primary antibodies against VCAM1

(mouse, 1:100; Santa Cruz), NeuN (neuron marker, 1:100; Chemicon, Temecula, CA, USA), glial fibrillary acidic protein (GFAP; astrocytes marker, 1:100; Sigma, St. Louis, MO, USA), CD11b (microglia marker, 1:100; Abcam, Cambridge, MA, USA) caspase-3 (rabbit, 1:100; Santa Cruz) and Bcl-2 (rabbit, 1:100; Santa Cruz) overnight at 4 °C, followed by a mixture of FITC- and TRITC-conjugated seconary antibodies (Jacks on ImmunoResearch) for 2 h at 4 °C. In order to detect the morphology of apoptotic cells, sections were covered with DAPI (0.1 mg/mL in PBS; Sigma) for 1 h at 30 °C. The stained sections were examined with Leica confocal microscope or Leica fluorescence microscope (Germany).

Terminal Deoxynucleotidyl Transferase-Mediated Biotinylated-dUTP Nick-End Labeling

Terminal deoxynucleotidyl transferase-mediated biotinylated-dUTP nick-end labeling (TUNEL) staining was performed using the In Situ Cell Death Detection Kit, Fluorescence (Roche Applied Science, Mannheim, Germany). Frozen tissue sections were rinsed with PBS and treated with 1 % Triton-100 in PBS for 2 min on ice. Slides were rinsed in PBS and incubated for 60 min at 37 °C with 50 lL of TUNEL reaction mixture. After washing with PBS, the slides were analyzed with fluorescence microscopy (Leica, DM 5000B; Leica CTR 5000; Germany).

Quantitative Analysis

Cell quantification was implemented in an unbiased manner. To avoid counting the same cell in more than one section, we counted every fifth section (50 μm apart). VCAM1-positive cells 2 mm from the hematoma center were counted at 400× magnification. For each section, three separate caudate putamen regions were examined. The cell counts in the three or four sections were then used to determine the total number of VCAM1-positive cells per square millimeter. The number of cells double-labeled for VCAM1 and the other phenotypic markers like NeuN, GFAP, and CD11b used in the experiment was quantified. To identify the proportion of NeuN-positive cells expressing VCAM1, a minimum of 200 NeuN positive cells were counted adjacent to the hematoma in each section. Then, double-labeled cells for VCAM1 and NeuN were recorded. Two or three adjacent sections per animal were sampled.

Statistical Analysis

All data were analyzed with Stata 7.0 statistics software. Values were expressed as mean ± SEM. Significance testing was performed using a one-way analysis of variance (ANOVA) to compare data from different experimental groups. $P < 0.05$ was considered to be statistically significant. Every experiment consisted of at least three replicates per condition.

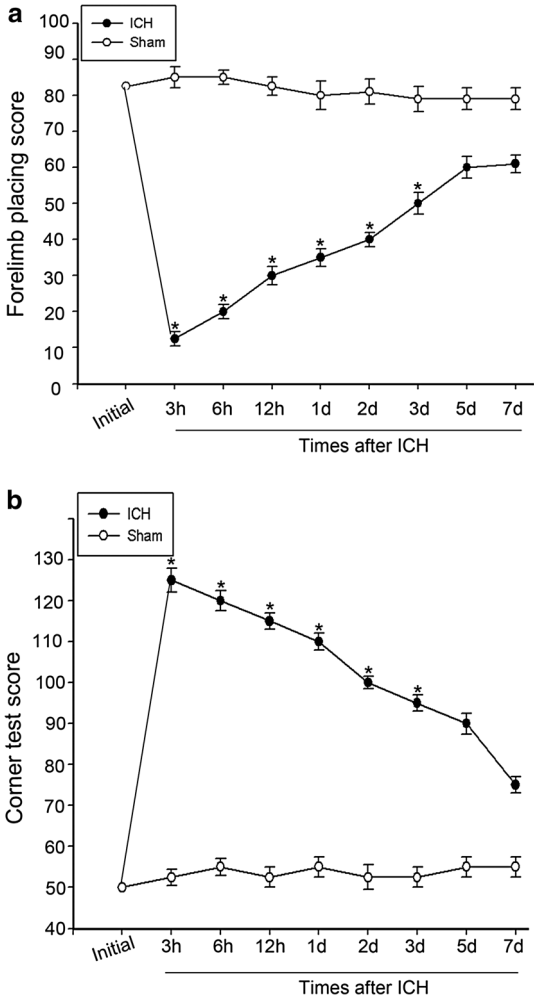

Fig. 1 Estimations and scores of behavioral tests on rats suffering from ICH. Behavioral tests were executed in rats after ICH or sham operation. Forelimb placing test (**a**) and corner turn test (**b**) scores at different survival times after ICH. Rats following ICH performed significantly worse compared with the sham group over the first 3 days (*asterisk* denotes $P < 0.05$) with no significant differences at baseline or 5 days later

Results

Neurological Deficits Following ICH in Adult Rats

To explore the expression and possible function of VCAM1 in rat models of unilateral brain injury such as ICH, we established an ICH model in adult rats and

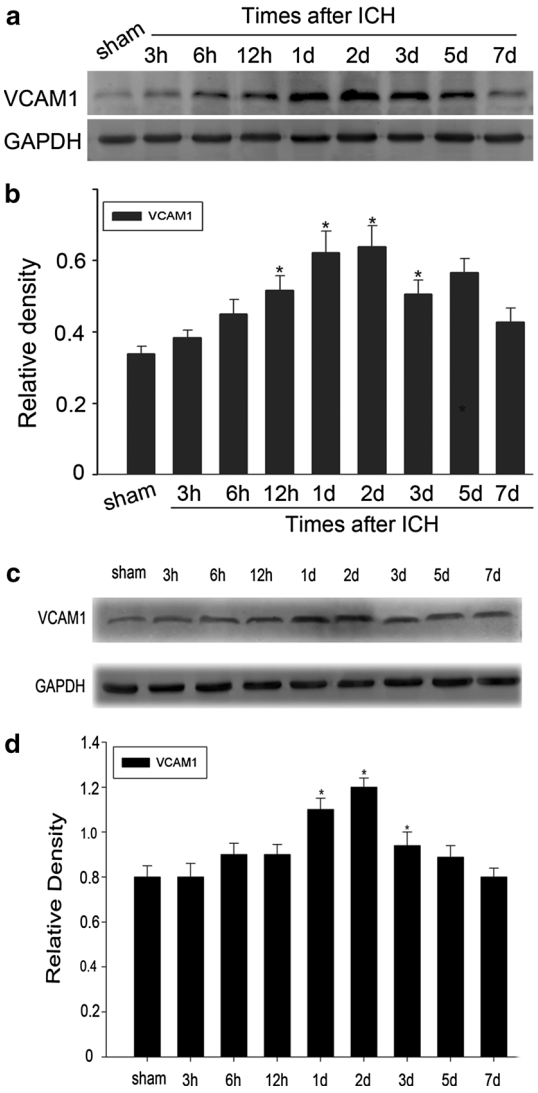

Fig. 2 Changes of VCAM1 protein expression following ICH. Western blot was performed to study the protein levels of VCAM1 surrounding the hematoma at various survival times. VCAM1 expression was relatively low in the sham group, increased gradually after ICH, peaked at day 2, and declined thereafter (**a**, **c**). **b**, **d** Quantification graphs (relative optical density) of the intensity of staining of VCAM1 and GAPDH at each time points. GAPDH was used to confirm that equal amount of protein was run on gel. The data are mean ± SEM (n = 3, $P < 0.05$, *asterisk* significantly different from the normal and sham groups)

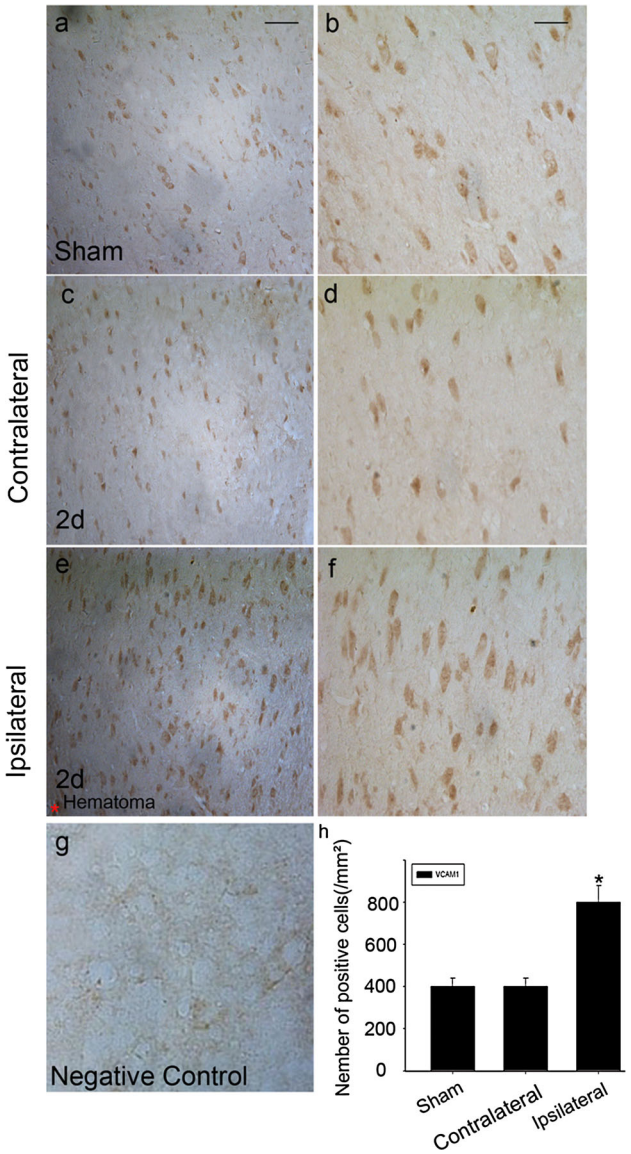

Fig. 3 Representative microphotographs for VCAM1 immunohistochemistry surrounding the hematoma. Low level of VCAM1 was detected in the sham group (**a**, **b**). At day 2 after ICH, the contralateral group showed no significant difference in VCAM1 (**c**, **d**) compared with the sham ones, while the ipsilateral group (**e**, **f**) showed increased VCAM1 expression (**e**, **f**). No positive signals were found in the negative control (**g**). The number of VCAM1 positive cells was largely increased comparing the ipsilateral group with the sham and contralateral groups (**h**). *Asterisk* denotes $P < 0.05$. *Scale bar*: *left column*, 50 μm; *right columns*, 10 μm

evaluated the changes in neurological functions following ICH. Rats in the sham and ICH groups were assessed with the forelimb placing and corner turn test at different survival times, respectively. The ICH group showed markedly impaired compared with the sham group over the first 3 days ($^*P < 0.05$). By 5 days and thereafter, both the forelimb placing and corner turn score gradually recovered to the baseline, indicating the functional recovery of the rat neurological deficits in rats (Fig. 1a, b).

Changes in Protein Expression of VCAM1 After ICH by Western Blot Analysis

To determine the total protein level of VCAM1 after ICH, protein extracts from rat brains were separated by SDS-PAGE and analyzed by western blot. As shown in (Fig. 2a, c), VCAM1 level was low in sham-control group.

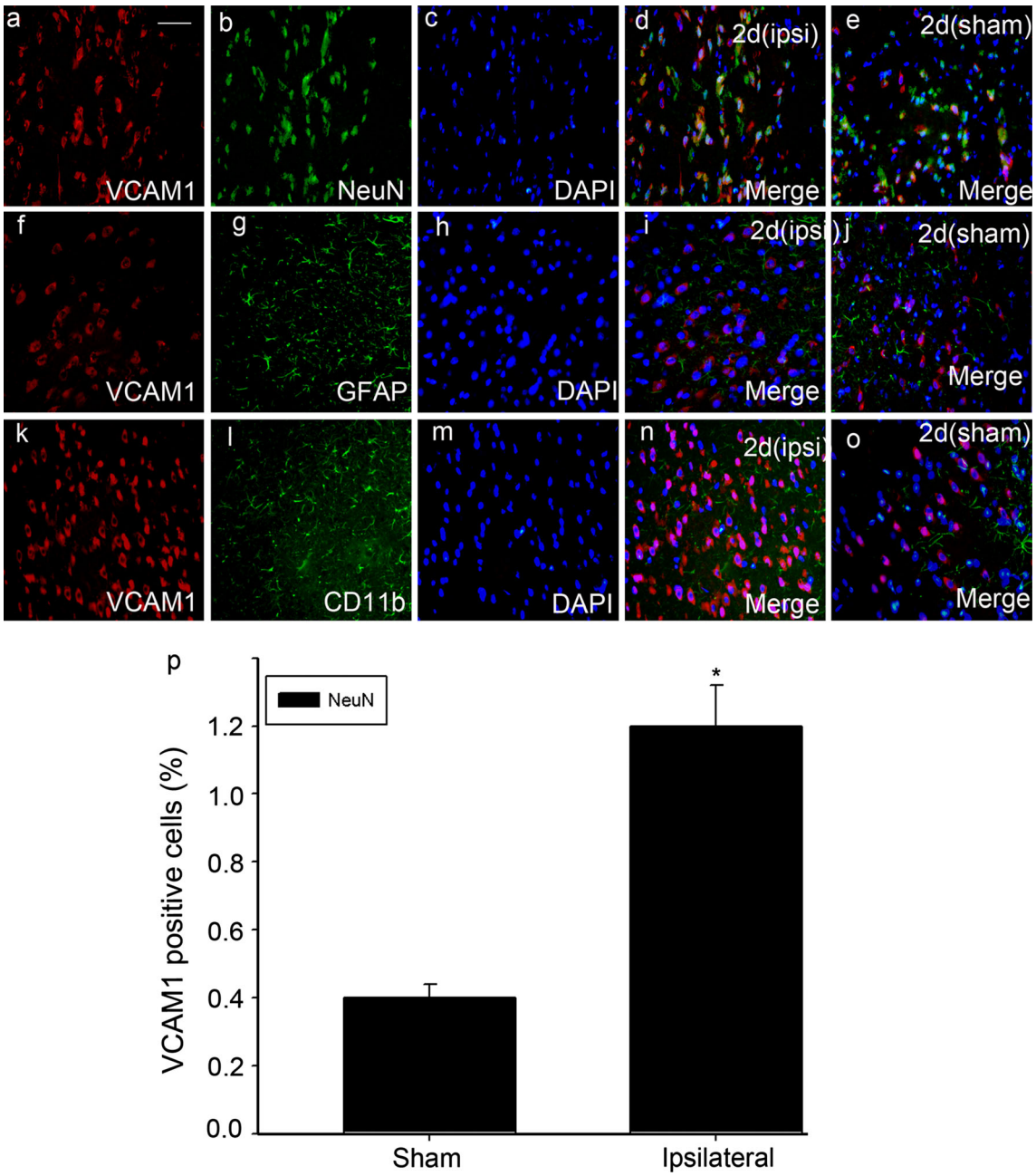

Fig. 4 The colocalization of VCAM1 with different cellular markers by double immunofluorescent staining. In the adult rat caudate within 3 mm distance from the hematoma at the second day after ICH, horizontal sections were labeled with VCAM1 (*Red* **a**, **f**, **k**), different cell markers (*Green* **b**, **g**, **l**) such as neuronal marker (NeuN), astrocyte marker (GFAP) and microglia marker (CD11b) as well as DAPI (*Blue* **c**, **h**, **m**) to show the nucleus. The *yellow* and *white color* visualized in the merged images represented the colocalization of VCAM1 with different phenotype-specific markers (**d**, **e**) and the *purple* indicated the colocalization of the nucleus with phenotype-specific markers (**d**, **e**, **i**, **j**, **n**, **o**). Colocalization of VCAM1 with different phenotype-specific markers in the sham group (**e**, **j**, **o**) were shown in the caudate. Quantitative analysis of NeuN-positive cells expressed VCAM1 (%) in the sham group and 2 days after ICH. (ipsi) indicates the perihematomal region and (sham) presents the sham group. *Asterisk* indicates significant difference at $P < 0.05$ compared with the sham group (**p**). *Error bars* represent SEM. *Scale bars* 20 μm (**a**) (Color figure online)

Standardizing densitometry against GAPDH showed that the total level of VCAM1 has a significant up-regulation from 12 h post ICH operation, peaked at day 2 and then gradually decreased to the normal level ($P < 0.01$, Fig. 2b, c). (Figure 2a, the antibody was purchased from Santa Cruz; Fig. 2b, the antibody was purchased from Sigma-Aldrich). These findings revealed that the expression of VCAM1 undergoes a substantial alteration after rat ICH.

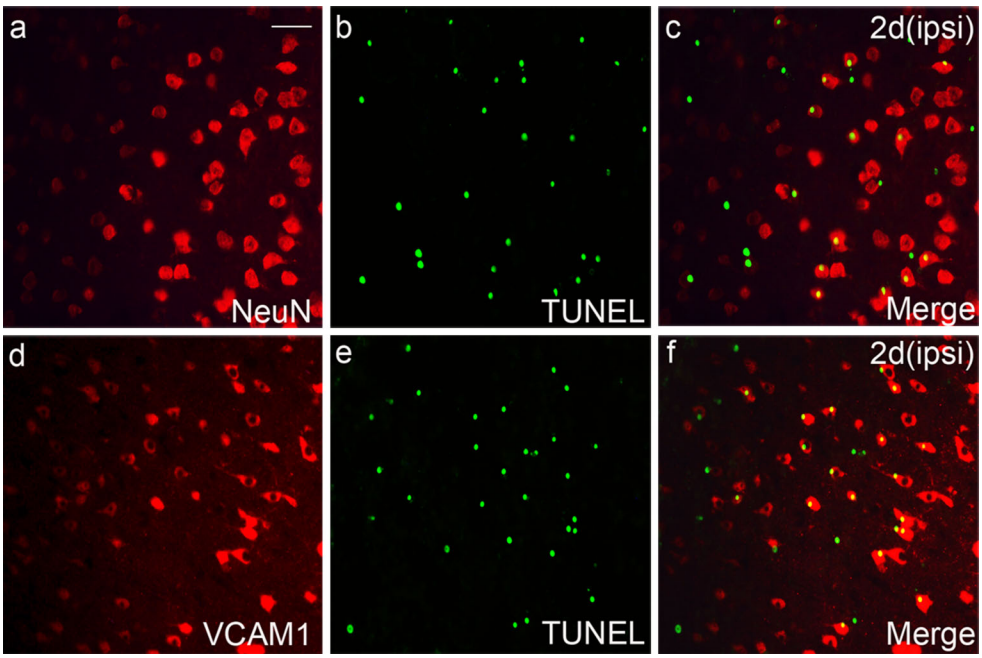

Fig. 5 Detection of neuronal apoptosis and VCAM1 expression after ICH. TUNEL staining showed VCAM1 was relevant to neuronal apoptosis after ICH (**a**–**f**). The *yellow* color (visualized in the merged images) represented colocalization of NeuN (*red*, **a**)/VCAM1 (*red*, **d**) and TUNEL positive cells (*green*, **b**, **e**) at day 2 after ICH. (*ipsi*) indicates perihematomal region. *Scale bars* 20 μm (**a**) (Color figure online)

The Distribution Changes of VCAM1 Immunoreactivity in the Perihematomal Region After ICH

To determine the distribution of VCAM1 after ICH, we performed immunohistochemistry 2 days after ICH. The sham group showed a low level of VCAM1 staining (Fig. 3a, b), similar to the profiles in the contralateral side of the experimental brains (Fig. 3c, d). The immunostaining of VCAM1 observably increased in the brain tissue surrounding the hematoma at day 2 after ICH (Fig. 3e, f, h) and these results were consistent with Western blot results. No staining was observed in the negative control (Fig. 3g).

Phenotype of VCAM1-Positive Cells

To further investigate the cell type expressing VCAM1 after ICH, double immunofluorescent microscopy was used with different cell type markers: NeuN, GFAP, and CD11b, which are markers of neurons, astrocytes and microglia respectively. In the sham group, the expression of VCAM1 was mainly restricted in neurons, and little in astrocytes and microglia (Fig. 4e, j, o). After ICH, enhanced VCAM1 positive signals found in neurons around the hematoma (Fig. 4d). And we observed that VCAM1 was still hardly co-labled with GFAP and CD11b (Fig. 4i, n). To identify the proportion of NeuN-positive cells expressing VCAM1, a minimum of 200 phenotype-specific marker positive cells were counted between the sham and 2 days after ICH groups (Fig. 4p). VCAM1 expression was markedly increased in neurons (the NeuN-positive cells) after ICH compared with the sham group, which were consistent with the results of immunohistochemistry staining. And the localizations of VCAM1 appeared to be confined mainly to the cytoplasm of neurons. The expression and distribution of VCAM1 in NeuN positive cells indicated that VCAM1 might be associated with the changes of biological function of neurons after ICH.

Association of VCAM1 with Neuronal Apoptosis After ICH

Increasing evidence suggested that neuronal apoptosis occurred surrounding the hematoma after ICH [9, 23]. Based on previous observations, the variation of VCAM1 expression was mainly in neurons, accordingly we proposed VCAM1 might participate in the changes of neuronal biological functions like apoptosis. Neuronal apoptosis develops vital influence on various CNS diseases, such as ischemia stroke and intracerebral hemorrhage [24], which relates to complex and sophisticated pro-apoptotic and anti-apoptotic processes. But, the exact relationship between neuronal apoptosis and VCAM1 remains to be illuminated. In this study, TUNEL labeling was used to prove the involvement of VCAM1 in neuronal apoptosis

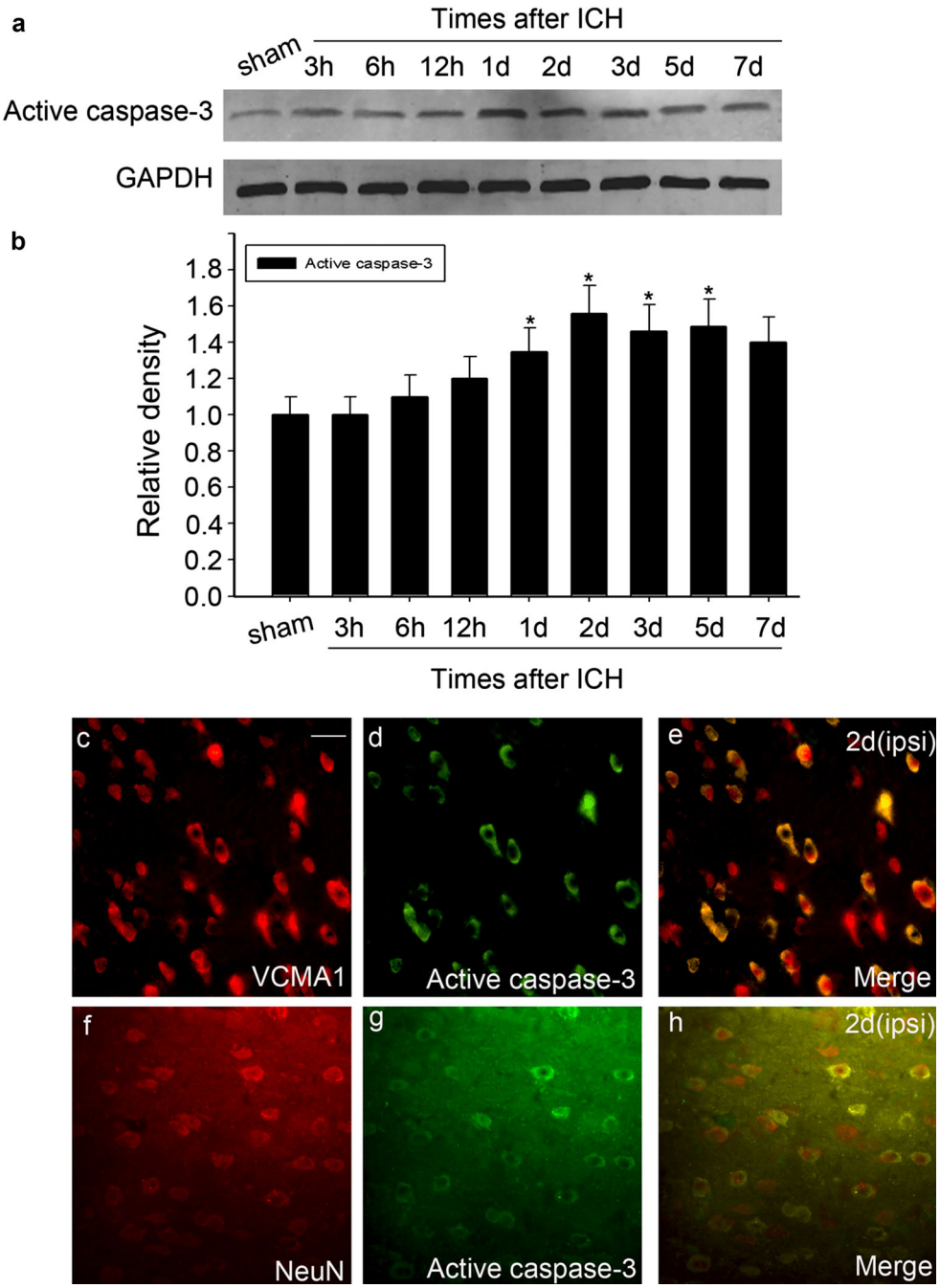

Fig. 6 Detection of neuronal apoptosis and relative VCAM1 changes after ICH. **a** Western blot analysis of active caspase-3 in brains after ICH. The expression of active caspase-3 increased after ICH and peaked at 2 days. GAPDH was used to confirm that equal amount of protein was run on gel. **b** Quantification graphs (relative optical density) of the intensity of staining of active caspase-3 and GAPDH at each time points. The data are mean ± SEM ($P < 0.05$, *asterisk* indicates significantly different from the normal group and sham group). In brain coronal slices within 3 mm distal to the hematoma, the colocalizations of active caspase-3 and VCAM1 (**e**) were detected. Moreover, there were colocalizations between the active caspase-3 and NeuN (**h**). (*ipsi*) indicates perihematomal region. *Scale bars* 20 μm (**c**) (Color figure online)

following ICH (Fig. 5a–f). As mentioned above, various mechanisms contribute to neuronal apoptosis after ICH. Among them, caspase-3 is always supposed to be the most important executioner caspase and has an intimate connection with both extrinsic and intrinsic apoptotic pathways. We also examined the protein level of active caspase-3 and its co-localization with VCAM1 in rat ICH model. The expression of active caspase-3 increased after ICH and peaked at day 2 (Fig. 6a, b). Additionally, the co-localizations of VCAM1/active caspase-3 in addition to active caspase-3/NeuN (Fig. 6c) manifested that VCAM1 might participate in neuronal apoptosis after ICH. Furthermore, western blot was performed to examine the expression of Bcl-2, and p53 (Fig. 7a, b). The level of Bcl-2 significantly decreased after ICH, and the increased expression of p53 was temporally correlated with VCAM1 expression. Taken together, these results indicated that VCAM1 might play a crucial role in neuronal apoptosis via a caspase-3-dependent pathway after ICH, which might be regulated by p53 (Fig. 7c–h).

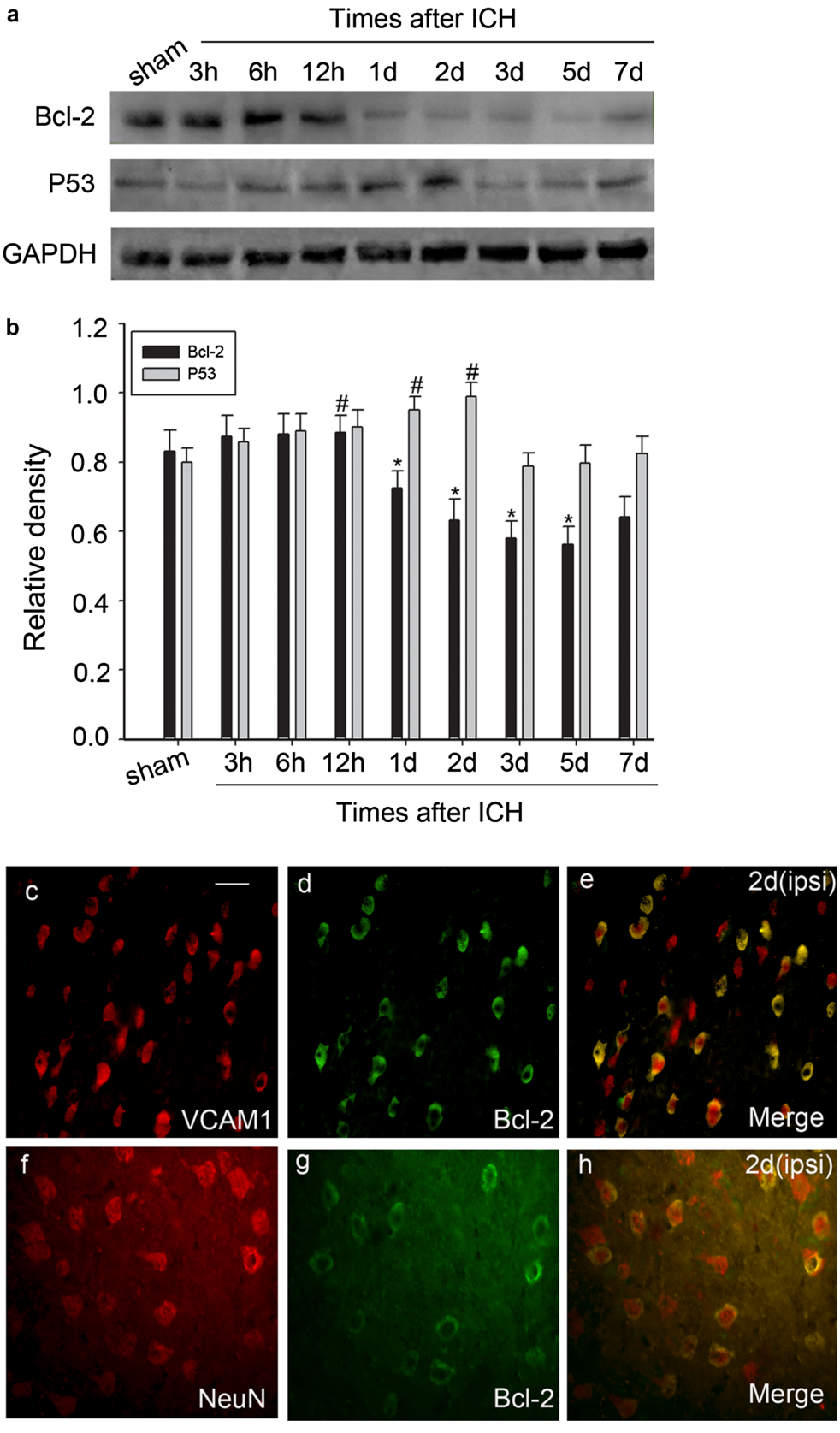

Fig. 7 Detection of the relationship between VCAM1 and Bcl-2 after ICH. Protein expression of p53 and Bcl-2 after traumatic brain injury. (**b**) The *bar chart* showed the ratio of p53 and Bcl-2 to GAPDH at each time point; these data are mean ± SEM (n = 3, $*P < 0.05$, *asterisk* indicates significantly different from the sham group). The colocalizations of VCAM1/NeuN and Bcl-2 were also detected by double immunofluorescent staining in the perihematomal region (**e**, **h**). (*ipsi*) indicates the perihematomal region. *Scale bars* 20 μm (Color figure online)

Discussion

The present study mimicked clinical ICH in adult rats to evaluate the role of VCAM1 after ICH by performing a controlled autologous blood injection [19, 20]. The rats suffering from ICH displayed significantly functional damage assessed by behavioral testing. Western blot analysis and immunohistochemistry revealed that VCAM1 was strikingly up-regulated in the perihematomal region 2 days after ICH. Double immunofluorescence labeling implicated that VCAM1 was mainly co-located with neurons, but not astrocytes or microglia. At the same time, there was a parallel up-regulation of active-caspase-3 and p53 with that of VCAM1 in a time-dependent manner. Consistent with previous studies, the expression of anti-apoptotic gene Bcl-2 was reduced time-dependently following ICH. Based on our data, VCAM1 might be associated with neuronal apoptosis after ICH.

Intracerebral hemorrhage is a devastating event, carrying a very high morbidity and mortality rate, so getting a much clearer conception about the underlying molecular and cellular mechanisms of damage following ICH is imminent for both individuals and societies [25]. Experimental animal ICH models are capable to reproduce the general important pathophysiologic events documented in human ICH, including edema development, dramatically reduced metabolism, and tissue pathologic responses [26]. Hence, ICH models serve as an important tool for new understanding of the fundamental mechanisms of brain injury after an intracerebral bleed. Previous researches provide the evidence of neuronal apoptosis in ICH and show a vital role of apoptosis in the whole ICH pathological process. Mitochondria are involved in the so-called intrinsic pathway of apoptosis where they release soluble proteins, including cytochrome c, from the intermembrane space to initiate caspase activation in the cytosol [27]. The release of these proteins is a result of the integrity of the mitochondrial outer membrane (OMM) being compromised. The process is called mitochondrial outer membrane permeabilization (MOMP). MOMP is under the control of the pro-apoptotic Bcl-2 family members. Bcl-2 family protein Bax and Bak are constitutively inserted into the OMM by a C-terminal transmembrane domain, then form lipidic pores wide enough for cytochrome c to release and induce MOMP [28]. It is commonly accepted that, as a famous tumor suppresser gene, p53 may mediate neuronal apoptosis after ICH [29]. After suffering from damage, transactivation of p53 is up-regulated and subsequently accelerates the transcription of some specific target genes [30]. Among them, Bax, Noxia, and the BH-3 only protein PUMA may induce mitochondrial membrane permeabilization changes, release cytochrome c from the inner mitochondrial members; Soon afterwards form an apoptosome, create a platform to assemble the initiator molecules of intrinsic apoptotic pathway; ultimately induce apoptosis via activate-caspase-3 [31, 32]. Caspase-3 is always known as the most important executioner and has an intimate correlation with both extrinsic and intrinsic apoptotic pathways.

Vascular cell adhesion molecule 1 (CD106) is one of the major vascular adhesion mediators directing the immune response. It is also a member of the immunoglobulin family that combines to integrin 1β and VLA4 and occurs on the memory T-cells [33]. In addition, up-regulation of VCAM1 could exert a protective role in maintaining the integrity of the ependymal zone in the process of inflammation [13]. At low concentration, ICAM-1 (CD54) and VCAM-1 (CD106) act synergistically with anti-IgM, in inhibiting apoptosis in the germinal center (GC) [34]. Also, VCAM-1 delays neutrophil apoptosis and maintains physiologic function though direct ligation of the integrin receptor $\alpha_9\beta_1$ [35]. CD106 inhibited SCL-induced up-regulation of Bcl-x_L and rescued B cells from apoptosis [36]. These all reveal that VCAM1 may play a role in the apoptosis. However, the molecular mechanisms that VCAM1 regulates apoptosis and its possible correlation with neuronal apoptosis after ICH remain to be explored.

Our present study proved that the expression of VCAM1 was strikingly increased around the hematoma, which indicated that VCAM1 might be involved in the physiological and pathological processes following ICH. And our data certificated the involvement of VCAM1 in neuronal apoptosis following ICH. Based on our data, it might provide a novel way to explore the underlying molecular and cellular mechanisms of CNS after ICH and afford a special target for the treatment of ICH. Nevertheless, further studies remains to be done to seek the underlying cellular and molecular mechanisms and therapeutic potentials of VCAM1 for ICH, in order to achieving a better prognosis following ICH.

Acknowledgments This work was supported in part by National Natural Science Foundation of China (31444003, 312700802, 31170766); Nantong City Social Development Projects funds (HS2012032); Natural science foundation of the Jiangsu higher education institutions (11KJA310002); A Project Funded by the Priority Academic Program Development of Jiangsu Higher Education Institutions (PAPD).

References

1. van Asch CJ, Luitse MJ, Rinkel GJ, van der Tweel I, Algra A, Klijn CJ (2010) Incidence, case fatality, and functional outcome of intracerebral haemorrhage over time, according to age, sex, and ethnic origin: a systematic review and meta-analysis. Lancet Neurol 9(2):167–176. doi:10.1016/S1474-4422(09)70340-0
2. Feigin VL, Lawes CM, Bennett DA, Barker-Collo SL, Parag V (2009) Worldwide stroke incidence and early case fatality reported

in 56 population-based studies: a systematic review. Lancet Neurol 8(4):355–369. doi:10.1016/S1474-4422(09)70025-0
3. Qureshi AI, Mendelow AD, Hanley DF (2009) Intracerebral haemorrhage. Lancet 373(9675):1632–1644. doi:10.1016/S0140-6736(09)60371-8
4. Candelise L, Gattinoni M, Bersano A, Micieli G, Sterzi R, Morabito A (2007) Stroke-unit care for acute stroke patients: an observational follow-up study. Lancet 369(9558):299–305. doi:10.1016/S0140-6736(07)60152-4
5. Terent A, Asplund K, Farahmand B, Henriksson KM, Norrving B, Stegmayr B, Wester PO, Asberg KH, Asberg S (2009) Stroke unit care revisited: who benefits the most? A cohort study of 105,043 patients in Riks-Stroke, the Swedish Stroke Register. J Neurol Neurosurg Psychiatry 80(8):881–887. doi:10.1136/jnnp.2008.169102
6. Crandall KM, Rost NS, Sheth KN (2011) Prognosis in intracerebral hemorrhage. Rev Neurol Dis 8(1–2):23–29
7. Aronowski J, Zhao X (2011) Molecular pathophysiology of cerebral hemorrhage: secondary brain injury. Stroke 42(6):1781–1786. doi:10.1161/STROKEAHA.110.596718
8. Bradl M, Lassmann H (2010) Oligodendrocytes: biology and pathology. Acta Neuropathol 119(1):37–53. doi:10.1007/s00401-009-0601-5
9. Gong C, Boulis N, Qian J, Turner DE, Hoff JT, Keep RF (2001) Intracerebral hemorrhage-induced neuronal death. Neurosurgery 48(4):875–882 Discussion 882–873
10. Sukumari-Ramesh S, Alleyne CH Jr, Dhandapani KM (2012) Astrocyte-specific expression of survivin after intracerebral hemorrhage in mice: a possible role in reactive gliosis? J Neurotrauma 29(18):2798–2804. doi:10.1089/neu.2011.2243
11. Kitamura Y, Shimohama S, Kamoshima W, Ota T, Matsuoka Y, Nomura Y, Smith MA, Perry G, Whitehouse PJ, Taniguchi T (1998) Alteration of proteins regulating apoptosis, Bcl-2, Bcl-x, Bax, Bak, Bad, ICH-1 and CPP32 in Alzheimer's disease. Brain Res 780(2):260–269
12. Liu X, Kim CN, Yang J, Jemmerson R, Wang X (1996) Induction of apoptotic program in cell-free extracts: requirement for dATP and cytochrome c. Cell 86(1):147–157
13. Kokovay E, Wang Y, Kusek G, Wurster R, Lederman P, Lowry N, Shen Q, Temple S (2012) VCAM1 is essential to maintain the structure of the SVZ niche and acts as an environmental sensor to regulate SVZ lineage progression. Cell Stem Cell 11(2):220–230. doi:10.1016/j.stem.2012.06.016
14. Osborn L, Hession C, Tizard R, Vassallo C, Luhowskyj S, Chi-Rosso G, Lobb R (1989) Direct expression cloning of vascular cell adhesion molecule 1, a cytokine-induced endothelial protein that binds to lymphocytes. Cell 59(6):1203–1211
15. Chen Q, Zhang XH, Massague J (2011) Macrophage binding to receptor VCAM-1 transmits survival signals in breast cancer cells that invade the lungs. Cancer Cell 20(4):538–549. doi:10.1016/j.ccr.2011.08.025
16. Damiano JS, Cress AE, Hazlehurst LA, Shtil AA, Dalton WS (1999) Cell adhesion mediated drug resistance (CAM-DR): role of integrins and resistance to apoptosis in human myeloma cell lines. Blood 93(5):1658–1667
17. Bao M, Chen Z, Xu Y, Zhao Y, Zha R, Huang S, Liu L, Chen T, Li J, Tu H, He X (2012) Sphingosine kinase 1 promotes tumour cell migration and invasion via the S1P/EDG1 axis in hepatocellular carcinoma. Liver Int 32(2):331–338. doi:10.1111/j.1478-3231.2011.02666.x
18. Qin W, Lu Y, Zhan C, Shen T, Dou L, Man Y, Wang S, Xiao C, Bian Y, Li J (2012) Simvastatin suppresses apoptosis in vulnerable atherosclerotic plaques through regulating the expression of p(53), Bcl-2 and Bcl-xL. Cardiovasc Drugs Ther 26(1):23–30. doi:10.1007/s10557-011-6347-z
19. Xue M, Del Bigio MR (2003) Comparison of brain cell death and inflammatory reaction in three models of intracerebral hemorrhage in adult rats. J Stroke Cerebrovasc Dis 12(3):152–159. doi:10.1016/S1052-3057(03)00036-3
20. Yang S, Song S, Hua Y, Nakamura T, Keep RF, Xi G (2008) Effects of thrombin on neurogenesis after intracerebral hemorrhage. Stroke 39(7):2079–2084. doi:10.1161/STROKEAHA.107.508911
21. Karabiyikoglu M, Hua Y, Keep RF, Ennis SR, Xi G (2004) Intracerebral hirudin injection attenuates ischemic damage and neurologic deficits without altering local cerebral blood flow. J Cereb Blood Flow Metab 24(2):159–166. doi:10.1097/01.WCB.0000100062.36077.84
22. Hua Y, Schallert T, Keep RF, Wu J, Hoff JT, Xi G (2002) Behavioral tests after intracerebral hemorrhage in the rat. Stroke 33(10):2478–2484
23. Xi G, Keep RF, Hoff JT (2006) Mechanisms of brain injury after intracerebral haemorrhage. Lancet Neurol 5(1):53–63. doi:10.1016/S1474-4422(05)70283-0
24. Calio ML, Marinho DS, Ko GM, Ribeiro RR, Carbonel AF, Oyama LM, Ormanji M, Guirao TP, Calio PL, Reis LA, Simoes Mde J, Lisboa-Nascimento T, Ferreira AT, Bertoncini CR (2014) Transplantation of bone marrow mesenchymal stem cells decreases oxidative stress, apoptosis, and hippocampal damage in brain of a spontaneous stroke model. Free Radic Biol Med 70:141–154. doi:10.1016/j.freeradbiomed.2014.01.024
25. Rymer MM (2011) Hemorrhagic stroke: intracerebral hemorrhage. MO Med 108(1):50–54
26. Andaluz N, Zuccarello M, Wagner KR (2002) Experimental animal models of intracerebral hemorrhage. Neurosurg Clin N Am 13(3):385–393
27. Vaux DL (2011) Apoptogenic factors released from mitochondria. Biochim Biophys Acta 1813(4):546–550. doi:10.1016/j.bbamcr.2010.08.002
28. Martinou JC, Youle RJ (2011) Mitochondria in apoptosis: Bcl-2 family members and mitochondrial dynamics. Dev Cell 21(1):92–101. doi:10.1016/j.devcel.2011.06.017
29. Ke K, Li L, Rui Y, Zheng H, Tan X, Xu W, Cao J, Xu J, Cui G, Xu G, Cao M (2013) Increased expression of small heat shock protein alphaB-crystallin after intracerebral hemorrhage in adult rats. J Mol Neurosci 51(1):159–169. doi:10.1007/s12031-013-9970-2
30. Miller FD, Pozniak CD, Walsh GS (2000) Neuronal life and death: an essential role for the p53 family. Cell Death Differ 7(10):880–888. doi:10.1038/sj.cdd.4400736
31. Cregan SP, MacLaurin JG, Craig CG, Robertson GS, Nicholson DW, Park DS, Slack RS (1999) Bax-dependent caspase-3 activation is a key determinant in p53-induced apoptosis in neurons. J Neurosci 19(18):7860–7869
32. Jurgensmeier JM, Xie Z, Deveraux Q, Ellerby L, Bredesen D, Reed JC (1998) Bax directly induces release of cytochrome c from isolated mitochondria. Proc Natl Acad Sci USA 95(9):4997–5002
33. Seyedmajidi M, Shafaee S, Bijani A, Bagheri S (2013) VCAM1 and ICAM1 expression in oral lichen planus. Int J Mol Cell Med 2(1):34–40
34. Koopman G, Keehnen RM, Lindhout E, Newman W, Shimizu Y, van Seventer GA, de Groot C, Pals ST (1994) Adhesion through the LFA-1 (CD11a/CD18)-ICAM-1 (CD54) and the VLA-4 (CD49d)-VCAM-1 (CD106) pathways prevents apoptosis of germinal center B cells. J Immunol 152(8):3760–3767
35. Ross EA, Douglas MR, Wong SH, Ross EJ, Curnow SJ, Nash GB, Rainger E, Scheel-Toellner D, Lord JM, Salmon M, Buckley CD (2006) Interaction between integrin alpha9beta1 and vascular cell adhesion molecule-1 (VCAM-1) inhibits neutrophil apoptosis. Blood 107(3):1178–1183. doi:10.1182/blood-2005-07-2692
36. Kim HR, Kim KW, Kim BM, Jung HG, Cho ML, Lee SH (2014) Reciprocal activation of CD4+T cells and synovial fibroblasts by stromal cell-derived factor 1 promotes RANKL expression and osteoclastogenesis in rheumatoid arthritis. Arthritis Rheumatol 66(3):538–548. doi:10.1002/art.38286